Chinese Chemical Letters 35 (2024) 109539

Contents lists available at ScienceDirect

Chinese Chemical Letters

journal homepage: www.elsevier.com/locate/cclet

Construction of pyrene-based hydrogen-bonded organic frameworks as photocatalysts for photooxidation of styrene in water

Rongxin Zhu[1], Shengsheng Yu[1,*], Xuanzong Yang, Ruyu Zhu, Hui Liu, Kaikai Niu, Lingbao Xing*

School of Chemistry and Chemical Engineering, Shandong University of Technology, Zibo 255000, China

ARTICLE INFO

Article history:
Received 19 October 2023
Revised 12 January 2024
Accepted 18 January 2024
Available online 28 January 2024

Keywords:
Pyrene
Hydrogen-bonded organic frameworks
Singlet oxygen
Photocatalysis
Styrene

ABSTRACT

Using hydrogen-bonded organic frameworks (HOFs) as photosensitizers to perform photocatalytic oxidation reactions under green and mild conditions is still a challenge for the application of HOFs materials. This study presents a novel approach that exploits HOFs to enhance the efficiency of photocatalytic oxidation for achieving visible light catalytic oxidation of styrene and its derivatives in the aqueous environment. By using 1,3,6,8-tetrakis(*p*-benzoic acid)pyrene (H_4TBAPy) as the monomer, a pyrene-based hydrogen-bonded organic framework (PFC-1) with a microporous structure was successfully prepared. Compared with monomer H_4TBAPy, due to the exciton effect and the interlayer confinement of HOFs, the singlet oxygen ($^1O_2$) production efficiency is significantly improved, which has great potential in photocatalytic oxidation reactions. Subsequently, the practicality of PFC-1 as a photocatalyst was studied, and the photocatalytic oxidation of styrene and its derivatives in aqueous solution was achieved under visible light with high catalytic efficiency, indicating that PFC-1 has significant potential to promote photocatalytic oxidation reactions under mild conditions. The utilization of HOFs as photosensitizers in this straightforward approach enables the attainment of green photocatalytic oxidation, hence expanding the potential applications of HOFs materials within the realm of photocatalysis.

Hydrogen-bonded organic frameworks (HOFs) are a type of organic porous materials formed by the self-assembly of organic monomers through intermolecular hydrogen-bonding interactions. The significant interest garnered by HOFs can be attributed to their favourable characteristics, including gentle synthesis conditions, excellent biocompatibility, high porosity, low density, and excellent repeatability [1–9]. In recent years, HOFs have gained significant prominence and have found extensive applications in several fields such as photocatalysis [10–12], gas storage and separation[13–20], biomedicine [21], sensing [22–27], and proton conduction [28–30]. Typically, the stability of HOFs is primarily influenced by hydrogen bonding to a limited extent. The development of a stable HOFs requires the incorporation of non-covalent interactions, including π-π interactions, dipole-dipole interactions, and van der Waals forces. In contrast to the extensively studied metal-organic frameworks (MOFs) [31–33] and covalent organic frameworks (COFs) [34,35] that have garnered significant interest in the realm of materials research, HOFs have not been widely employed in conventional catalytic applications, although possessing numerous appealing characteristics. The practical utilization of these applications continues to be impeded by challenges such as intermolecular charge transfer, site stability, and the limited directionality and pH stability associated with the existence of hydrogen bonds [36]. On the other hand, directing attention towards mild photooxidation catalysis proves to be a more advantageous option for applications of HOFs. This is particularly true when employing visible light as the medium, as it represents one of the least harsh methods for HOFs to attain organic photocatalysis applications [37].

Previous studies have shown that porous organic materials, such as MOFs [38–40], COFs [41–43], exhibit notable photooxidation capabilities. In recent years, there has been a surge in research efforts focused on the development of high-throughput HOFs with the primary objective of fabricating catalytically active porous materials. The utilization of grid structures presents numerous advantages in relation to the manageability and replicability of the solution. The aforementioned benefits arise from the enhanced porosity, diverse structural composition, adaptable functionality, and the relatively weak hydrogen bonding interactions observed in HOFs. When comparing HOFs with inorganic semiconductor materials, it becomes evident that HOFs possess notable benefits. Nevertheless, there is a scarcity of literature about the investigation of

* Corresponding authors.
E-mail addresses: ssyu@sdut.edu.cn (S. Yu), lbxing@sdut.edu.cn (L. Xing).
[1] These authors contributed equally to this work.

https://doi.org/10.1016/j.cclet.2024.109539
1001-8417/

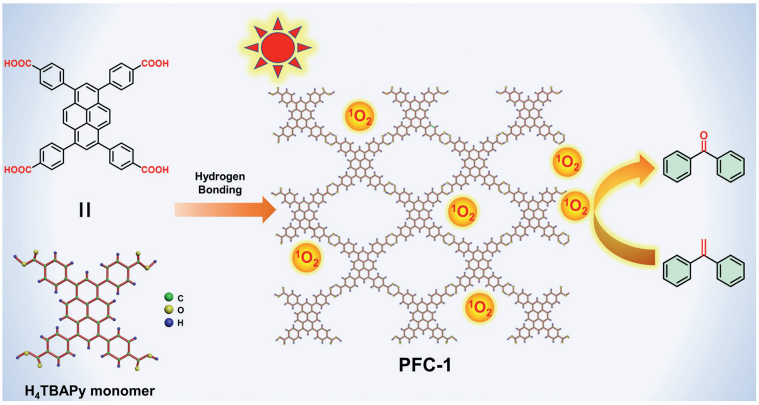

Scheme 1. Schematic diagram of the construction of PFC-1 and the photooxidation reactions.

HOFs in the realm of organic photocatalysis. Wang and coworkers constructed HOFs based on guanine-modified naphthalene diimide molecules through hydrogen bonding interactions, which can efficiently generate singlet oxygen ($^1O_2$) in methanol under red light and exhibit good photocatalytic oxidation activity for thioanisoles [44]. Very recently, Cao and coworkers present a novel approach that utilizes HOF monomers directly for the purpose of effective photoredox catalysis, eliminating the need for catalyst prefabrication. Surprisingly, this basic model demonstrates comparable efficiency to prefabricated high-activity, selective, and versatile HOFs catalysts in the context of photocatalytic sulfides oxidation [45]. Nevertheless, the utilization of HOFs as photocatalysts has been restricted not only to specific types of photocatalytic reactions, but also to organic or mixed solvents as reaction media. Therefore, it is imperative to advance the development of gentle photocatalytic reactions using HOFs in water, as well as broaden the range of organic reactions that can be facilitated by photocatalysis.

The present investigation employed 1,3,6,8-tetrakis(*p*-benzoic acid)-pyrene as an organic monomer for the purpose of self-assembling into a hydrogen-bonded organic framework (PFC-1). The pore architectures of PFC-1 were confirmed by the X-ray diffraction (XRD) and N_2 adsorption-desorption experiments. It is noteworthy that the inclusion of a pyrene unit with a conjugated structure in the monomer has advantageous effects on enhancing the π-π interactions between molecules, which leaded to an improvement in the stability of the HOFs. Furthermore, as compared to the monomer H_4TBAPy, the framework structure exhibits a stronger interlayer arrangement with the constraint effect, which has a notable impact on enhancing the production efficiency of $^1O_2$. Subsequently, we conducted an investigation into the utilization of PFC-1 as a photocatalyst for the process of photooxidation reaction of 1,1-diphenylethylene. By optimizing several factors such as reaction duration, excitation wavelength, and choice of solvents, we achieved notable improvements in the reaction yield. Specifically, we successfully conducted the photooxidation of 1,1-diphenylethylene in an aqueous solution using visible light, resulting in a remarkably high yield of 92%. Under identical experimental conditions, PFC-1 has demonstrated the ability to selectively catalyze the oxidation of styrene and its derivatives (Scheme 1). Furthermore, to confirm the universality of PFC-1 as a photosensitizer for facilitating photocatalytic oxidation reactions, the photooxidative coupling of 2,4,6-trimethylaniline was successfully accomplished through visible light catalysis, resulting in a yield of 85%. This result represents the significant potential of PFC-1 as a photosensitizers for promoting mild photocatalytic oxidation reactions in water.

PFC-1 was constructed by adjusting the precipitation conditions of H_4TBAPy through introducing methanol into *N,N*-dimethylformamide (DMF) solution (Scheme S1 in Supporting information) [46–49]. The scanning electron microscopy (SEM) technique was employed to observe and analyze the morphology and size of the PFC-1. The results indicated that the PFC-1 exhibited a rod-shaped morphology, with an average length ranging of 1–3 μm (Fig. 1a). XRD was employed to characterize the crystal structure of PFC-1. The produced XRD pattern (Fig. 1b) exhibits a sequence of peaks that align with the simulated patterns and PFC-1 as reported in prior studies [48,49]. Moreover, it can be seen that the decarboxylation reaction did not take place when PFC-1 was successful preparation. This observation was supported by the analysis of the fourier transform infrared spectroscopy (FTIR), where the presence of the carboxylic acid group was indicated by the peak at around 1690 cm^{-1} (Fig. S1 in Supporting information). Subsequently, the porosity of PFC-1 was measured through N_2 adsorption-desorption experiments. The N_2 adsorption-desorption isotherms of PFC-1, as depicted in Fig. 1c, exhibits a type I isotherm, thereby confirming the presence of microporous properties. Furthermore, the BET surface area of PFC-1 is measured to be 910 m^2/g, whereas the pore volume is determined to be 0.59 cm^3/g. Moreover, the pore size distribution diagram is examined using the non-local density functional theory (NLDFT) model. The primary pore diameter of the fabricated material ranges from approximately 1.1 nm to 1.41 nm (Fig. 1d). As a result, the aforementioned findings suggest that the synthesis of PFC-1 was accomplished effectively.

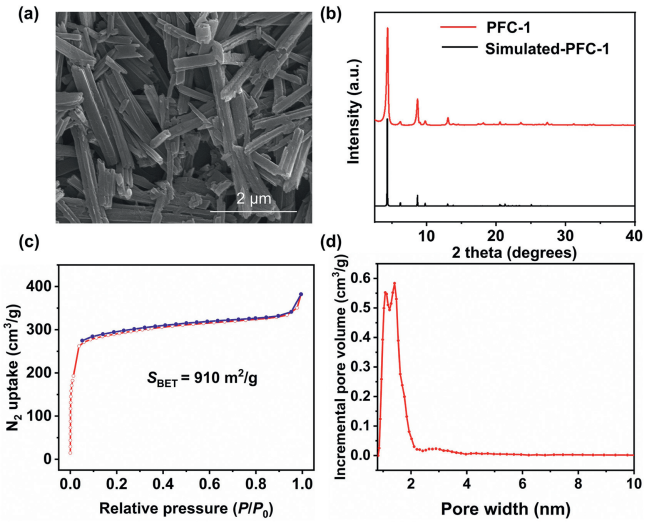

Fig. 1. (a) SEM image of PFC-1. (b) XRD patterns of simulated PFC-1 and PFC-1. (c) N_2 adsorption-desorption isotherms of PFC-1. (d) NLDFT pore size distribution of PFC-1.

Table 1
Optimization of photooxidation reaction conditions.[a,b]

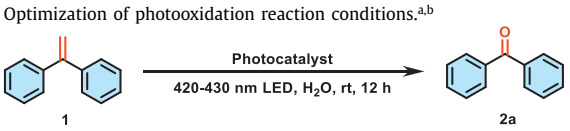

Entry	Dariation from standard conditions[a]	Yield[b] (%)
1	None	92
2	H_4TBAPy instead of PFC-1	18
3	PFC-1 (2.5 mg) instead of PFC-1 (5 mg)	49
4	PFC-1 (10 mg) instead of PFC-1 (5 mg)	94
5	6 h instead of 12 h	45
6	24 h instead of 12 h	95
7	CH_3CN instead of H_2O	77
8	CH_2Cl_2 instead of H_2O	45
9	CH_3OH instead of H_2O	65
10	THF instead of H_2O	51
11	DMF instead of H_2O	43
12	DMSO instead of H_2O	48
13	DMA instead of H_2O	45
14	390–400 nm LED instead of 420–430 nm LED	77
15	400–410 nm LED instead of 420–430 nm LED	80
16	410–420 nm LED instead of 420–430 nm LED	85
17	430–440 nm LED instead of 420–430 nm LED	83
18	465–475 nm LED instead of 420–430 nm LED	60
19	Without PFC-1	No reaction
20	Without light	No reaction

[a] Reaction standard conditions: 1,1-diphenylethylene (0.2 mmol), PFC-1 (5 mg), H_2O (3 mL), 420–430 nm LED (10 W), room temperature, air, 12 h.
[b] Isolated yields.

Table 2
Substrate scope with respect to styrene derivatives.[a,b]

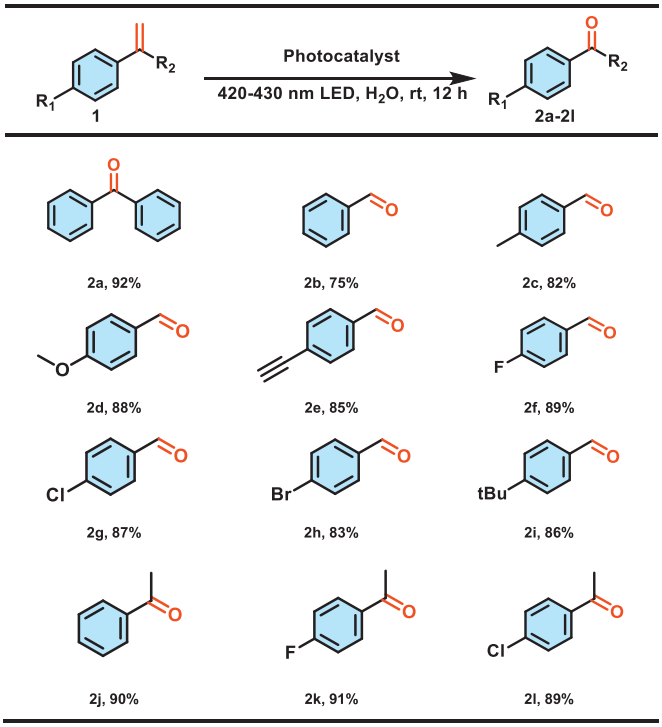

[a] Reaction conditions: styrene derivatives (0.2 mmol), PFC-1 (5 mg), H_2O (3 mL), 420–430 nm LED (10 W), room temperature, air, 12 h.
[b] Isolated yields.

The optical properties of H_4TBAPy and PFC-1 were studied through UV–vis absorption and fluorescence emission spectroscopy. As depicted in Fig. S2a (Supporting information), the absorption peaks of PFC-1 exhibited a noteworthy red-shift in comparison to the H_4TBAPy monomers. This observation suggests that the luminescent monomers of H_4TBAPy in PFC-1 were organized in a face-to-face arrangement, resulting in the formation of J-shaped aggregates. The fluorescence emission of the H_4TBAPy monomers is observed to be feeble, however, a notable enhancement in emission is observed upon the self-assembly of these monomers into a novel hydrogen-bonded organic framework known as PFC-1 (Fig. S2b in Supporting information). In addition, we also measured the fluorescence quantum yield of H_4TBAPy monomers and PFC-1, the formation of HOFs leads to the increase of fluorescence quantum yield from 8.6% (H_4TBAPy) to 11.8% (PFC-1).

To assess the capacity of PFC-1 in generating reactive oxygen species (ROS) in an aqueous solution, a particular indicator for $^1O_2$ known as 9,10-anthracenediyl-bis(methylene)dimalonic acid (ABDA) was employed. The compound ABDA exhibits preferential reactivity towards $^1O_2$, leading to a corresponding reduction in its absorbance. Upon illumination at a wavelength range of 420–430 nm, it was noticed that the absorption peak of ABDA decreased in the presence of PFC-1. Furthermore, the rate of $^1O_2$ production by PFC-1 was found to be notably higher than that of H_4TBAPy monomers, as shown in Figs. S3 and S4 (Supporting information). In addition, the generation of $^1O_2$ were further investigated by electron-spin resonance (ESR) measurements upon adding 2,2,6,6-tetramethylpiperidine (TEMP) to the solution of PFC-1 as the spin trapping agent. No ROS signal is detected without the irradiation. Under the irradiation of 420–430 nm LED, the signal of $^1O_2$ was detected, which indicates PFC-1 has an excellent ability to generate $^1O_2$ (Fig. S5 in Supporting information).

In order to further study the application of PFC-1 as photosensitizers in photocatalytic oxidation reactions, 1,1-diphenylethylene was used as a template substrate to explore the photooxidation reaction. As shown in Table 1, the photocatalytic oxidation reaction of 1,1-diphenylethylene can occur efficiently and gives a yield of 92% in water (entry 1, Fig. S6 in Supporting information). If the photocatalyst is changed to H_4TBAPy monomers, the reaction yield is reduced to 18% (entry 2). If the amount of catalyst is reduced, the reaction yield will be reduced to 49% (entry 3). Conversely, an increase in the quantity of catalyst has a negligible effect on the reaction yield, with a yield of around 94% (entry 4). Reducing the reaction time to 6 h will reduce the reaction yield to 45% (entry 5). Conversely, increasing the reaction time to 24 h has a minimal effect on the reaction yield, with a yield of 95% (entry 6). The alteration of the reaction solvent from water to CH_3CN, CH_2Cl_2, CH_3OH, tetrahydrofuran (THF), DMF, dichlorosulfoxide (DMSO), or *N,N*-dimethylacetamide (DMA) will result in varying degrees of reduction in the reaction yields (entries 7–13, 77%, 45%, 65%, 51%, 43%, 48%, and 45%). When the light wavelength range of 420–430 nm is altered to 390–400 nm, 400–410 nm, 410–420 nm, 430–440 nm, and 465–475 nm, the resulting reaction yields decrease to 77%, 80%, 85%, 83%, and 60% accordingly (entries 14–18). In the absence of a photocatalyst or light, the reaction does not take place, so suggesting that both a photocatalyst and light are essential prerequisites for the reaction to proceed effectively (entries 19 and 20). In order to confirm the practicality of pyrene-based HOFs as a photocatalyst for oxidation of styrene, HOF-100 and HOF-102 has been studied under the same conditions. As shown in Table S1 (Supporting information), when HOF-100 and HOF-102 act as photocatalysts, the photocatalytic oxidation reaction of 1,1-diphenylethylene can occur efficiently and gives a yield of 84% and 86%, respectively, which is slightly lower than PFC-1. These results proved the universality of HOFs with pyrene rings for photooxidation of styrene.

In order to assess the applicability of PFC-1 as a photocatalyst for the enhancement of photooxidation of styrene and its derivatives in aqueous solution, a range of substrates were employed for the photooxidation reactions. As shown in Table 2, styrene could be successfully oxidized to benzaldehyde (**2b**) in 75% yield

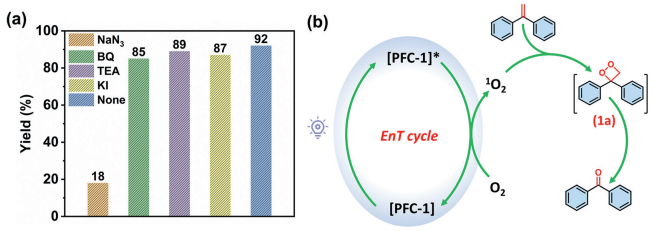

Fig. 2. (a) Controlled experiments of 1,1-diphenylethylene photooxidation in the presence of different scavengers. (b) Proposed mechanism for photooxidation of 1,1-diphenylethylene.

under standard conditions (Fig. S7 in Supporting information). In addition, the system demonstrated high efficiency in facilitating reactions involving substrates containing electron-donating groups (-CH_3 and –OCH_3), in which the yields of substrates were found to be 82% (**2c**) and 88% (**2d**), respectively (Figs. S8 and S9 in Supporting information). The substrate containing alkynyl substituent also give a high yield of 85% (**2e**, Fig. S10 in Supporting information). Similarly, styrene derivatives containing electron-withdrawing groups (-F, -Cl, -Br) also showed successful reactions with high yields (89% for **2f**, 87% for **2g**, and 83% for **2h**, Figs. S11-S13 in Supporting information). Substrate containing tert–butyl substituent also exhibited excellent yield of 86% (**2i**, Fig. S14 in Supporting information). In addition, PFC-1 also has high photocatalytic efficiencies for isopropenylbenzene and its derivatives (90% for **2j**, 91% for **2k**, and 89% for **2l**, Figs. S15-S17 in Supporting information). These results all demonstrate the significant potential of PFC-1 to promote the photooxidation reaction of styrene derivatives under mild conditions. To demonstrate the stability of PFC-1 in the photocatalytic oxidation reaction, XRD was employed. We recovered the PFC-1 which completed the photocatalytic oxidation reaction of 1,1-diphenylethylene under standard conditions. After washing and drying, we re-conducted the XRD experiment, and the results showed that the structure of PFC-1 did not change significantly (Fig. S18 in Supporting information), which proved the stability of PFC-1 in the photocatalytic oxidation reaction.

In order to explore the mechanism and active substances of the photooxidation reaction of styrene and its derivatives, we have employed four free radical scavengers 1,4-benzoquinone (BQ), triethylamine (TEA), potassium iodide (KI) and sodium azide (NaN_3) to capture the photogenerated superoxide anion radicals ($O_2^{\bullet-}$), hydroxyl radicals ($^{\bullet}OH$), holes (h^+) and singlet oxygen ($^1O_2$). As shown in Fig. 2a, the introduction of NaN_3 resulted in a significant decrease in the yield of the 1,1-diphenylethylene photooxidation reaction, which was only 18% of the yield. However, under the same reaction conditions, the addition of BQ, TEA, and KI had no significant effect on the reaction yield, indicating that $^1O_2$ is the main active species in the photooxidation reaction of styrene and its derivatives. Based on the experimental results and previous literature [50,51], the reaction mechanism of the styrene photooxidation reaction was proposed (Fig. 2b). Under light irradiation, PFC-1 is excited from the ground state [PFC-1] to the excited state [PFC-1]*. Subsequently, the energy of [PFC-1]* is transferred to oxygen, resulting in the generation of $^1O_2$ and [PFC-1]. The substrate then interacts with $^1O_2$ to form the intermediate substance 1a, and finally form the target product.

Furthermore, to enhance the understanding of the mechanism underlying the oxidation of styrene and its derivatives by $^1O_2$, and to confirm the broad use of PFC-1 as a type II photosensitizer in facilitating photocatalytic oxidation. PFC-1 was employed as the photosensitizers to investigate the photooxidative coupling reaction of 2,4,6-trimethylaniline in an aqueous medium. The yield of the photooxidative coupling reaction of 2,4,6-trimethylaniline by using PFC-1 as photocatalysts was observed to be 85% under identical reaction conditions (Table S2 and Fig. S19 in Supporting information). In contrast, the yield was found to be 23% by using H_4TBAPy monomer for the same reaction. This result provides additional evidence supporting the broad applicability of PFC-1 as photosensitizers in mild photocatalytic oxidation reactions. The active species of the photooxidative coupling reaction of 2,4,6-trimethylaniline was investigate by four free radical scavengers BQ, TEA, KI and NaN_3 to capture the photogenerated $O_2^{\bullet-}$, $^{\bullet}OH$, h^+ and $^1O_2$. As shown in Fig. S20 (Supporting information), the introduction of NaN_3 resulted in a significant decrease in the yield of the 2,4,6-trimethylaniline photooxidation reaction, which was only 16% of the yield. However, under the same reaction conditions, the addition of BQ, TEA, and KI had no significant effect on the reaction yield, indicating that $^1O_2$ is the main active species in the photooxidative coupling reaction of 2,4,6-trimethylaniline.

In summary, a rod-shaped PFC-1 with a microporous structure was constructed by using H_4TBAPy as the monomers. In contrast to the H_4TBAPy monomer, PFC-1 exhibits enhanced efficiency in generating $^1O_2$ as a result of the exciton effect and interlayer limitation inside its self-assembled hydrogen bonded frameworks, which makes PFC-1 has great application prospect in photocatalytic oxidation reaction. In this study, we suggest employing PFC-1 as photosensitizers to accomplish photocatalytic oxidation under mild conditions, which not only exhibit notable efficiency, specificity, and adaptability in the photocatalytic oxidation of styrene and its derivatives in water, but also utilized as photosensitizers to facilitate the photooxidative coupling of 2,4,6-trimethylaniline. This study presents novel opportunities for the utilization of HOFs as an environmentally friendly photosensitizers, expanding the potential applications of HOFs materials within the realm of photocatalysis.

Declaration of competing interest

The authors declare that they have no known competing financial interests or personal relationships that could have appeared to influence the work reported in this paper.

Acknowledgments

We are grateful for the financial support from the National Natural Science Foundation of China (No. 52205210) and the Natural Science Foundation of Shandong Province (Nos. ZR2020MB018, ZR2022QE033 and ZR2021QB049).

Supplementary materials

Supplementary material associated with this article can be found, in the online version, at doi:10.1016/j.cclet.2024.109539.

References

[1] I. Hisaki, C. Xin, K. Takahashi, T. Nakamura, Angew. Chem. Int. Ed. 58 (2019) 11160–11170.
[2] B. Wang, R.B. Lin, Z. Zhang, et al., J. Am. Chem. Soc. 142 (2020) 14399–14416.
[3] X. Gao, W. Lu, Y. Wang, et al., Sci. China Chem. 65 (2022) 2077–2095.
[4] P. Li, M.R. Ryder, J.Fraser Stoddart, Acc. Mater. Res. 1 (2020) 77–87.
[5] Z. Zhang, Y. Ye, S. Xiang, B. Chen, Acc. Chem. Res. 55 (2022) 3752–3766.
[6] W.K. Qin, C.H. Tung, L.Z. Wu, J. Mater. Chem. A 11 (2023) 12521–12538.
[7] D. Yu, H. Zhang, J. Ren, X. Qu, Chem. Soc. Rev. 52 (2023) 7504–7523.
[8] J. Gao, Y. Cai, X. Qian, et al., Angew. Chem. Int. Ed. 133 (2021) 20563–20569.
[9] Y. Cai, P.J. Gao, J.H. Li, et al., Angew. Chem. Int. Ed. 135 (2023) e202308579.
[10] J. Wang, Y. Mao, R. Zhang, et al., Adv. Sci. 9 (2022) 2204036.
[11] N. Zhong, M. Chen, Y. Luo, et al., Chem. Eng. J. 355 (2019) 731–739.
[12] B. Yu, L. Li, S. Liu, et al., Angew. Chem. Int. Ed. 60 (2021) 8983–8989.
[13] Y. He, S. Xiang, B. Chen, J. Am. Chem. Soc. 133 (2011) 14570–14573.
[14] H. Wang, B. Li, H. Wu, et al., J. Am. Chem. Soc. 137 (2015) 9963–9970.
[15] P. Li, Y. He, Y. Zhao, et al., Angew. Chem. Int. Ed. 54 (2015) 574–577.
[16] L. Chen, Z. Yuan, H. Zhang, et al., Angew. Chem. Int. Ed. 61 (2022) e202213959.
[17] Y. Li, X. Wang, H. Zhang, et al., Angew. Chem. Int. Ed. 62 (2023) e202311419.
[18] Y.L. Li, E.V. Alexandrov, Q. Yin, et al., J. Am. Chem. Soc. 142 (2020) 7218–7224.

[19] S. Nandi, D. Chakrabortya, R. Vaidhyanathan, et al., Chem. Commun. 52 (2016) 7249–7252.
[20] X.Z. Luo, X.J. Jia, J.H. Deng, et al., J. Am. Chem. Soc. 135 (2013) 11684–11687.
[21] X.T. He, Y.H. Luo, D.L. Hong, et al., ACS Appl. Nano Mater. 2 (2019) 2437–2445.
[22] H.Y. Li, S.Q. Zhang, M.L. Chen, et al., Anal. Chem. 94 (2022) 15448–15455.
[23] B. Wang, R. He, L.H. Xie, et al., J. Am. Chem. Soc. 142 (2020) 12478–12485.
[24] X. Xu, J. Wang, B. Yan, Adv. Funct. Mater. 31 (2021) 2103321.
[25] Z. Fan, S. Zheng, H. Zhang, et al., Chin. Chem. Lett. 33 (2022) 4317–4320.
[26] L. Tong, Y. Lin, X. Kou, et al., Angew. Chem. Int. Ed. 62 (2023) e202218661.
[27] C. Wang, X. Song, Y. Wang, et al., Angew. Chem. Int. Ed. 62 (2023) e202311482.
[28] A. Karmakar, R. Illathvalappil, B. Anothumakkool, et al., Angew. Chem. Int. Ed. 55 (2016) 10667–10671.
[29] S.C. Pal, D. Mukherjee, R. Sahoo, et al., ACS Energy Lett. 6 (2021) 4431–4453.
[30] Z. Yang, Y. Zhang, W. Wu, et al., J. Membrane Sci. 664 (2022) 121118.
[31] L. Wang, H. Xu, J. Gao, J. Yao, Q. Zhang, Coord. Chem. Rev. 398 (2019) 213016.
[32] H.C. "Joe" Zhou, S. Kitagawa, Chem. Soc. Rev. 43 (2014) 5415–5418.
[33] N. Stock, S. Biswas, Chem. Rev. 112 (2012) 933–969.
[34] S.Y. Ding, W. Wang, Chem. Soc. Rev. 42 (2013) 548–568.
[35] X. Feng, X. Ding, D. Jiang, Chem. Soc. Rev. 41 (2012) 6010–6022.
[36] Z.J. Lin, S.A. Mahammed, T.F. Liu, et al., ACS Cent. Sci. 8 (2022) 1589–1608.
[37] Q. Zhou, Y. Guo, Y. Zhu, Nat. Catal. 6 (2023) 574–584.
[38] A. Dhakshinamoorthy, Z. Li, H. Garcia, Chem. Soc. Rev. 47 (2018) 8134–8172.
[39] S. Wang, X. Wang, Small 11 (2015) 3097–3112.
[40] T. Zhang, W. Lin, Chem. Soc. Rev. 43 (2014) 5982–5993.
[41] Y.N. Gong, X. Guan, H.L. Jiang, Coordin. Chem. Rev. 475 (2023) 214889.
[42] X. Wang, L. Chen, S.Y. Chong, et al., Nat. Chem. 10 (2018) 1180–1189.
[43] Q. Yang, M. Luo, K. Liu, H. Cao, H. Yan, Appl. Catal. B 276 (2020) 119174.
[44] H. Zhao, Z. Zhou, X. Feng, et al., Nano Res. 16 (2023) 8809–8816.
[45] J. Li, Q. Yin, S.Y. Gao, et al., ACS Sustain. Chem. Eng. 11 (2023) 4389–4397.
[46] K. Ma, P. Li, J.H. Xin, et al., Cell Rep. Phys. Sci. 1 (2020) 100024.
[47] B. Wang, X.L. Lv, J. Lv, et al., Chem. Commun. 56 (2020) 66–69.
[48] Q. Yin, Z. Peng, R.J. Sa, et al., Angew. Chem. Int. Ed. 57 (2018) 7691–7696.
[49] M.L. Lu, W. Huang, S. Gao, et al., Anal. Chem. 94 (2022) 15832–15838.
[50] U. Caudillo-Flores, M.J. Muñoz-Batista, A.B. Hungría, et al., Appl. Catal. B 245 (2019) 49–61.
[51] M. Tajuelo, D. Rodríguez, M.T. Baeza-Romero, Chemosphere 231 (2019) 276–286.